Kinetics of CH_2ClO Radical Reactions with O_2 and NO, and the Unimolecular Elimination of HCl†

Fuxiang Wu and Robert W. Carr*

Department of Chemical Engineering and Materials Science, University of Minnesota, Minneapolis, Minnesota 55455

Received: May 30, 2000; In Final Form: August 18, 2000

The kinetics of the title reactions were investigated at 5−35 Torr total pressure and 265−306 K by UV flash photolysis and time-resolved mass spectrometry. The CH_2ClO radical was generated by photolysis of NOCl in the presence of CH_3Cl, O_2, and NO. Atomic chlorine from NOCl photodissociation abstracted H from CH_3Cl and initiated oxidation of CH_2Cl radicals, leading to formation of CH_2ClO. The CH_2ClO radical reacted with both O_2 and NO, or underwent unimolecular elimination of HCl. The kinetics were determined from growth rates of HC(O)Cl and HCl. The rate coefficient of the $CH_2ClO + O_2$ reaction was found to be independent of pressure. The temperature dependence can be expressed as: $k(CH_2ClO + O_2) = (2.0 \pm 0.7) \times 10^{-12} \exp[-(934 \pm 128)/T]$ cm^3 molecule^{-1} s^{-1}. The rate coefficients for the $CH_2ClO + NO$ reaction were found to be independent of both pressure and temperature, with the value $k(CH_2ClO + NO) = (2.7 \pm 0.6) \times 10^{-12}$ cm^3 molecule^{-1} s^{-1}, obtained by averaging all rate coefficients determined over the experimental range of pressure and temperature. The rate coefficient for unimolecular elimination of HCl from CH_2ClO was found to be pressure dependent, and well into the falloff. The unimolecular rate coefficient at 10 Torr can be expressed as $(7.7 \pm 2.3) \times 10^9 \exp[-(4803 \pm 722)/T]$ s^{-1}.

Introduction

The CH_2ClO radical is an intermediate in the oxidation of CH_3Cl. Methyl chloride oxidation occurs at high temperature in chlorine-catalyzed oxidative pyrolysis of methane[1,2](natural gas) and in incineration and biomass burning, and it occurs at low temperature in the atmosphere.[3] Methyl chloride is the most prevalent halocarbon in the atmosphere, with a global average tropospheric abundance of 600 pptv.[4] The principal source of atmospheric CH_3Cl is the world's oceans, with volcanoes, incinerators, and vegetation burning also making contributions.[3] In the atmosphere, CH_2ClO may be formed from CH_2ClO_2 by reaction with HO_2, reaction with NO, and through the bimolecular self-reaction. The CH_2ClO_2 radicals are produced by reaction of OH with CH_3Cl, followed by addition of O_2 to the resulting CH_2Cl radical. This paper is concerned with reactions of CH_2ClO at relatively low temperatures. The 265−306 K experimental temperature range is characteristic of the lower troposphere.

Laboratory investigations of reaction products at or near 1 atm of air have shown that when CH_2ClO is formed by disproportionation of two CH_2ClO_2 radicals at 298 K, it reacts with O_2 to form HC(O)Cl in 90−95% yield.[5,6] At lower O_2 partial pressures CH_2ClO also eliminates HCl in a unimolecular reaction that competes with the $CH_2ClO + O_2$ reaction.[7,8] This unimolecular reaction is quite facile, occurring even at 264 K.[8] A transition state for HCl elimination has been found by semiempirical MNDO calculations,[9] although the computed barrier height of 18.9 kcal mol^{-1} is higher than an estimate of 8.6 ± 1.9 kcal mol^{-1} that was made from the temperature dependence of the relative rate coefficients of reactions 5 and 6.[8]

In previous work, we determined absolute values of k_5 and k_6 at 306 K and at pressures from 7.5 to 35 Torr by flash photolysis with time-resolved mass spectrometry.[10] The chloromethoxy radical was generated by reactions 1−4.

$$Cl_2 + h\nu \rightarrow 2Cl \quad (1)$$

$$Cl + CH_3Cl \rightarrow CH_2Cl + HCl \quad (2)$$

$$CH_2Cl + O_2 + M \rightarrow CH_2ClO_2 + M \quad (3)$$

$$2CH_2ClO_2 \rightarrow 2CH_2ClO + O_2 \quad (4)$$

The rate coefficients of reactions 5 and 6 were determined from observed growth rates of HC(O)Cl and HCl by nonlinear regression of the data from an 18-step reaction mechanism. Reaction 6 was found to be well into the unimolecular falloff.

$$CH_2ClO + O_2 \rightarrow HC(O)Cl + HO_2 \quad (5)$$

$$CH_2ClO \rightarrow HCl + HCO \quad (6)$$

This work was undertaken to determine the temperature dependence of k_5 and k_6 and to further characterize the pressure dependence of reaction 6 at 289 K. To our knowledge, the temperature dependence of the absolute values of k_5 and k_6 has not been reported. The CH_2ClO radical was formed by reaction of CH_2ClO_2 with NO, which is enough faster than reaction 4 that the HCl growth is kinetically first-order, and with excess O_2, the growth of HC(O)Cl is pseudo-first-order. Furthermore, it was found that CH_2ClO reacts with NO, and a kinetic investigation of that reaction is also reported here.

Experimental Section

The reaction kinetics were determined by UV flash photolysis with time-resolved mass spectrometry. A detailed description

† Part of the special issue "Harold Johnston Festschrift".

10.1021/jp001953m CCC: $20.00
Published on Web 10/11/2000

of the experimental techniques and procedures has been published previously[11,12] and is briefly described here. The quadrupole/electron ionization mass spectrometer was interfaced with a temperature-controlled photolysis reactor by a 50 μm pinhole. A 1 μs xenon flash lamp was repetitively pulsed at 5 Hz. The reactor was continuously purged by flow of the reaction mixture at a sufficient rate (about 7 cm/s) to completely sweep away the reaction products between flashes. Electron ionization energies from 15 to 30 eV were employed to reduce fragmentation. Current pulses from a Daly detector were preamplified, discriminated, and signal-averaged with a multichannel analyzer. The shortest analyzer dwell time was limited to 0.098 ms in order to obtain sufficient signal so that the number of flashes required for signal averaging is not excessively long. This limited the first-order rate coefficients to values no larger than 7×10^3 s^{-1}. Moreover, due to the influence of the molecular velocity distribution,[13] data recorded before 0.2 ms were excluded from processing. Also, the sweep of the purge flow imposed an additional decay rate on data acquired after 30 ms. The experiments were designed to avoid interference by these factors.

Atomic Cl, generated by photolysis of NOCl in a CH_3Cl/NOCl/O_2/NO gas mixture, initiated the reaction. NOCl is preferable to Cl_2 as the Cl atom source because secondary reactions of OH and HCO with Cl_2 regenerate Cl atoms during the course of the reaction,[10] and these would adversely influence the first-order kinetic analysis of the data. Secondary generation of Cl does not occur with NOCl as the Cl source, and the other photodissociation product, NO, is already present in deliberately added quantities. To limit the photodissociation of CH_3Cl, which absorbs appreciably below 200 nm, and consequent complications due to CH_3O_2 chemistry, a quartz flash lamp having a short wavelength transmission cutoff above 200 nm was used. Reactions 7, 2, 3, and 8 generated the CH_2ClO radical. The presence of NO makes formation of CH_2ClO much faster than the self-reaction $2CH_2ClO_2 \rightarrow 2CH_2ClO + O_2$, which was the method of generation used in our previous work.[10] It also makes possible a study the reaction of CH_2ClO with NO.

$$NOCl + h\nu \rightarrow NO + Cl \quad (7)$$

$$Cl + CH_3Cl \rightarrow CH_2Cl + HCl \quad (2)$$

$$CH_2Cl + O_2 + M \rightarrow CH_2ClO_2 + M \quad (3)$$

$$CH_2ClO_2 + NO \rightarrow CH_2ClO + NO_2 \quad (8)$$

The CH_2ClO then reacts with O_2 to form HC(O)Cl (reaction 5) and undergoes a three-center unimolecular elimination of HCl (reaction 6).[7,8,10] We found that CH_2ClO reacts with NO (reaction 9).

$$CH_2ClO + O_2 \rightarrow HC(O)Cl + HO_2 \quad (5)$$

$$CH_2ClO \rightarrow HCl + HCO \quad (6)$$

$$CH_2ClO + NO \rightarrow \text{products} \quad (9)$$

Mixtures of $CH_3Cl/O_2/N_2$ were prepared and stored in a glass bulb. Nitrosyl chloride was prepared by the reaction of NO with Cl_2.[14,15]

$$2NO + Cl_2 \rightarrow 2NOCl \quad (10)$$

A small excess of NO was used, consuming all of the Cl_2 and leaving the NOCl containing about 5% NO. The NOCl/NO mixture was stored in a glass bulb overnight before use. To avoid the oxidation of NO to NO_2, the NOCl/NO mixture was kept out of contact with O_2 until just before a run, when it was introduced into the reactor through a separate inlet line. Chloromethane of 99.5% stated purity was procured from Aldrich Chemical Co., Inc., and Cl_2 of 99.9% stated purity was supplied by Sigma. Chloromethane and Cl_2 were degassed before use. NO of 99.9% purity was obtained from Matheson while the Toll Co. supplied extra dry grade O_2 and N_2 of 99.9% purity.

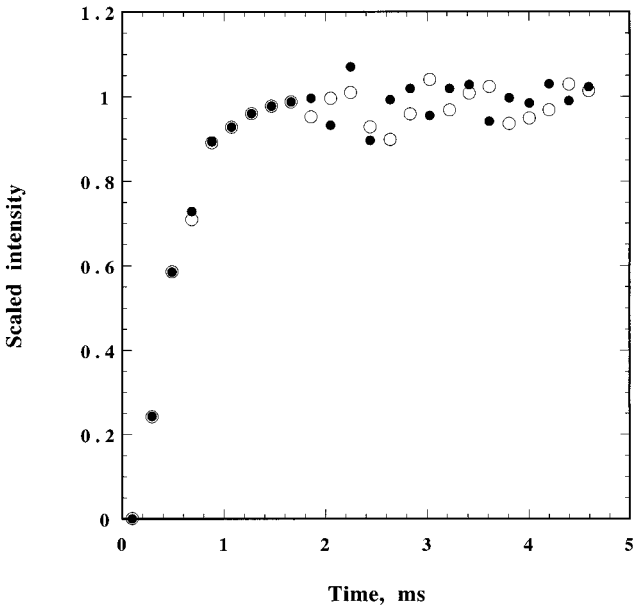

Figure 1. Experimental signals of HC(O)Cl and HCl at 289 K and 20 Torr. Gas mixture, 25% CH_3Cl/1.7% O_2 in N_2; [NO] = 4.24×10^{14} molecule cm^{-3}; [NOCl] = 3.34×10^{16} molecule cm^{-3}; ○, HC(O)Cl at $m/z = 64$; ●, HCl at $m/z = 36$.

The experiments were conducted at 5−35 Torr of total pressure at 289 K and at 10 Torr at 265, 280, and 306 K. The mole fraction of CH_3Cl in the $CH_3Cl/O_2/N_2$ mixture was normally about 25%. The concentrations of O_2 were in the range from 7×10^{15} to 4×10^{16} molecules cm^{-3}. The partial pressure of the NO/NOCl mixture was about 1 Torr for all experiments. The NO/NOCl mixtures give $(3-4) \times 10^{14}$ cm^{-3} of atomic chlorine upon flash photolysis. The mole fraction of NO in the NO/NOCl mixtures was set so that $[NO]/[CH_2Cl]_0$ was greater than 10 and the half time of reaction 8 was less than 90 μs. Under these experimental conditions the maximum half time for reaction 2 is less than 40 μs and the half time for reaction 3 is less than 100 μs. The CH_2ClO generation kinetics is well-separated from CH_2ClO decay kinetics. The concentration of HC(O)Cl was very low in many experiments, and 5000−10 000 flashes were usually needed for adequate signal-to-noise. The signal-to-noise ratio of HCl was much better than that of HC(O)Cl, due to higher absolute concentrations, and probably also due to better mass spectrometric detection sensitivity, although the latter point was not quantitatively addressed.

Results

Kinetic Analysis. Transient signals due to HC(O)Cl and HCl were detected. Figure 1 shows the normalized number of counts vs time for an experiment at 20 Torr and 289 K. The HC(O)Cl data are overlapped with those of HCl. We have previously shown that HC(O)Cl and HCl are products of reactions 5 and 6 and that the kinetics can be determined from measurements of their growth rates.[10] In the present investigation, reaction 9 also makes a contribution to HC(O)Cl. The rates of formation of HC(O)Cl and HCl were determined by monitoring $[COCl]^+$ at $m/z = 63$ or $[HCOCl]^+$ at $m/z = 64$, and $[HCl]^+$ at $m/z = 36$

and 38. No transient signals that could be attributed to CH_2ClO_2 or CH_2ClO were found. The background at $m/z = 63$ or 64 and at $m/z = 36$ or 38 was subtracted from the total HC(O)Cl and HCl ion counts, respectively. The background was obtained from the ion count in the first channel of the multichannel analyzer, which contains the background plus counts due to reactions occurring at times shorter than 0.098 ms. In the case of $m/z = 36$ or 38, the first channel contained the ion counts from prompt HCl arising from reaction 2, and possibly also from chemically activated CH_2ClO (see Discussion), in addition to instrumental background, so HCl from these sources is not present in Figure 1.

If reactions with O_2, NO, and HCl elimination are the only three processes competing for CH_2ClO radicals and if generation of CH_2ClO is sufficiently fast, the rate of disappearance of CH_2ClO can be expressed as

$$-\mathrm{d[RO]}/\mathrm{d}t = (k_5[\mathrm{O_2}] + k_6 + k_9[\mathrm{NO}])[\mathrm{RO}] \quad (11)$$

where [RO] is the concentration of CH_2ClO and k_9 is the overall rate coefficient for the NO + CH_2ClO reaction (see Discussion). Integrating eq 11 with the initial condition $[\mathrm{RO}] = [\mathrm{RO}]_0$, $t = 0$, and $[O_2]$ and [NO] constant gives

$$[\mathrm{RO}](t) = [\mathrm{RO}]_0 \exp\{-(k_5[\mathrm{O_2}] + k_6 + k_9[\mathrm{NO}])t\} \quad (12)$$

The formation rate of HC(O)Cl can be expressed as

$$\mathrm{d[HC(O)Cl]}/\mathrm{d}t = (k_5[\mathrm{O_2}] + k_9[\mathrm{NO}])[\mathrm{RO}](t) \quad (13)$$

Substitution of eq 12 into 13 and integration with the initial condition $[\mathrm{HC(O)Cl}] = 0$, $t = 0$, gives

$$[\mathrm{HC(O)Cl}](t) = \{(k_5[\mathrm{O_2}] + k_9[\mathrm{NO}])/\Sigma\}\,[\mathrm{RO}]_0\,[1 - \mathrm{e}^{-\Sigma t}] \quad (14)$$

where $\Sigma = k_5[\mathrm{O_2}] + k_6 + k_9[\mathrm{NO}]$. At $t = \infty$,

$$[\mathrm{HC(O)Cl}]_\infty = [\mathrm{RO}]_0\{(k_5[\mathrm{O_2}] + k_9[\mathrm{NO}])/\Sigma\} \quad (15)$$

and division of eq 14 by 15 gives, after rearrangement,

$$(1 - [\mathrm{HCOCl}]/[\mathrm{HCOCl}]_\infty) = \mathrm{e}^{-\Sigma t} \quad (16)$$

Equation 16 indicates that a plot of $\ln(1 - [\mathrm{H(O)Cl}]/[\mathrm{H(O)Cl}]_\infty)$ vs time should yield a straight line with a slope equal to $(k_5[\mathrm{O_2}] + k_6 + k_9[\mathrm{NO}])$, provided that O_2 and NO are present in sufficient excess that their concentrations can be taken to be constant. Figure 2 shows such a plot for data taken at 289 K and 20 Torr. The linearity supports the kinetic analysis. The value of $[\mathrm{HC(O)Cl}]_\infty$ was determined from the nearly flat later portion of the [HC(O)Cl] vs time curves, such as shown in Figure 1, which was taken to correspond to the asymptote. When the semilog plots include longer time data, there is increasing scatter of the data points as $[\mathrm{HC(O)Cl}]/[\mathrm{HC(O)Cl}]_\infty$ approaches unity. Therefore, the longer time (after 2 ms) data were not used to determine the first-order decay constants. Furthermore, eq 16 predicts that the intercept of the semilog plots should go through zero at $t = 0$. The failure to do so, which is apparent in Figure 2, is due to the formation of CH_2ClO, which is about 90% complete in $\leq$0.4 ms. A contribution is also made by the molecular velocity distribution, which distorts the concentration profile at these short times. For HCl formation, a similar analysis shows that

$$\ln(1 - [\mathrm{HCl}]/[\mathrm{HCl}]_\infty) = \{k_5[\mathrm{O_2}] + k_6 + k_9[\mathrm{NO}]\}t \quad (17)$$

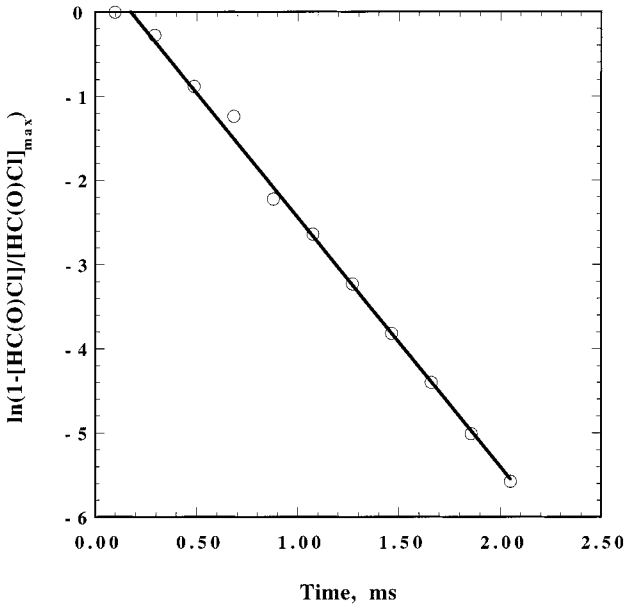

Figure 2. First-order plot of HC(O)Cl signal at 289 K and 20 Torr. Gas mixture, 25% CH_3Cl/1.7% O_2 in N_2; $[\mathrm{NO}] = 4.24 \times 10^{14}$ molecule cm^{-3}; $[\mathrm{NOCl}] = 3.34 \times 10^{16}$ molecule cm^{-3}; ○, experimental data; —, linear fit. $k' = 2956\ s^{-1}$ was obtained from this plot.

By comparing eqs 16 and 17 it is clear that determination of HCl growth rates gives the same information as HC(O)Cl growth rates. Under conditions where reactions 5 and 9 are pseudo-first-order, $k_5[\mathrm{O_2}] + k_6 + k_9[\mathrm{NO}]$ is a first-order overall CH_2ClO decay constant. Thus Σ is replaced by k' henceforth. First-order plots for HCl growth gave values of k' that were indistinguishable, within experimental error, from the k' determined from HC(O)Cl growth rates under the same experimental conditions.

Determination of k_5 and k_9. Values for the bimolecular rate coefficients k_5 and k_9 were extracted from the slopes, k', of the semilog plots by two experimental methods. In the first of these, HCl or HC(O)Cl growth curves were recorded at different partial pressures of O_2 by using $CH_3Cl/NOCl/O_2$ mixtures with different mole fractions of O_2, and fixed total pressure. The independently added NO partial pressure was kept constant and at a low value so that reaction 9 did not compete significantly with reaction 5, but yet reaction 8 was fast enough not to distort the kinetic growth curves. The kinetic analysis predicts that a plot of k' vs $[O_2]$ should have a slope equal to k_5 and an intercept of $k_6 + k_9[\mathrm{NO}]$. A second series of experiments was done at a specified temperature and pressure with mixtures of constant $CH_3Cl/NOCl/O_2$ mole fraction, and variable [NO]. The measured k' from these experiments were plotted vs [NO], and k_9 was determined from the slope. In this case, the intercept is $k_5[\mathrm{O_2}] + k_6$. These experiments were repeated at different total pressures and different temperatures to investigate the temperature and pressure dependence of the kinetics.

Figures 3 and 4 show the linearity of k' vs $[O_2]$ when [NO] is constant and of k' vs [NO] when $[O_2]$ is constant, respectively, at 289 K and at total pressures of 5, 10, 20, and 35 Torr. Experiments were also done at 15, 25, and 30 Torr. These are not shown in Figures 3 and 4 to avoid clutter. Similar plots were obtained at 10 Torr, only at other temperatures. Figure 3 shows that the range of $[O_2]$ in the k' vs $[O_2]$ plots decreased with increasing total pressure. Kinetic analysis (see Discussion section) shows that $[O_2]$ should be kept as low as possible to limit the complication caused by HO_2-related reactions. However, the minimum $[O_2]$ is limited by rate of reaction 3 to ensure

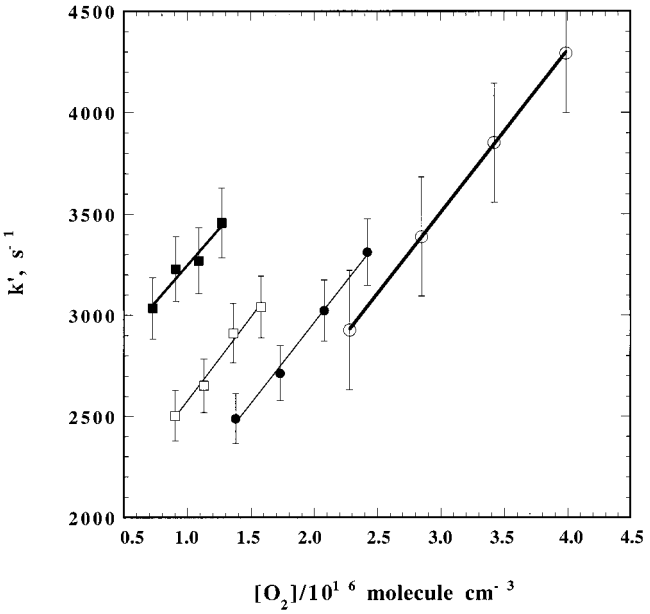

Figure 3. k' vs $[O_2]$ plots at 289 K and at different total pressures. Gas mixture, 25% CH_3Cl/O_2 in N_2; $[O_2] = (0.7-4) \times 10^{16}$ molecule cm^{-3}; $[NO] = 3.34 \times 10^{14}$ molecule cm^{-3}; $[NOCl] = 3.34 \times 10^{16}$ molecule cm^{-3}; ○, 5 Torr; ●, 10 Torr; □, 20 Torr; ■, 35 Torr.

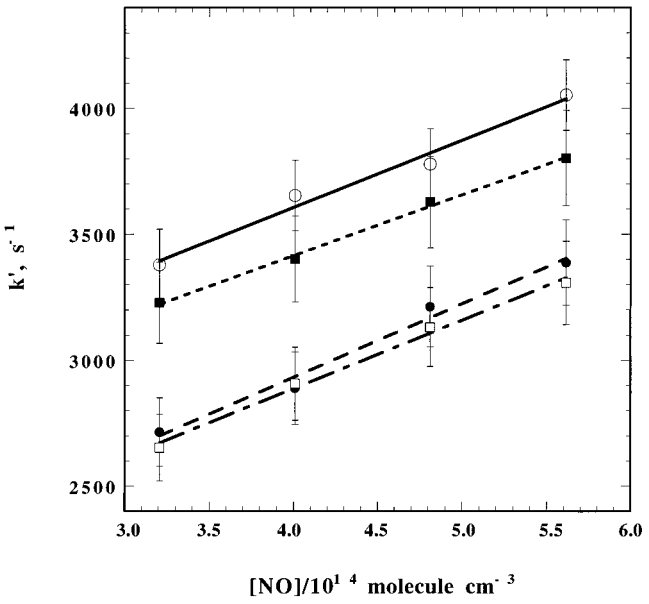

Figure 4. k' vs [NO] plot at 280 K and at different total pressures. Gas mixture, 25% $CH_3Cl/1.5\%$ O_2 in N_2; $[NO] = (3.2-5.6) \times 10^{14}$ molecule cm^{-3}; $[NOCl] = 3.34 \times 10^{16}$ molecule cm^{-3}; ○, 5 Torr; ●, 10 Torr; □, 20 Torr; ■, 35 Torr.

that its half time is less thane 0.1 ms. Since the rate coefficient of reaction 3 is pressure dependent, lower $[O_2]$ is allowed for the higher total pressure experiment. The time resolution of the experimental apparatus set an upper limit of k', which then limits $[O_2]$ at different temperatures and pressures so that the formation of HC(O)Cl by reaction 5 is not too fast. Although the feasible $[O_2]$ range is narrow in these experiments, these data support the pressure independence of k_5. The slopes in Figure 4 are also invariant with pressure, indicating that k_9 is independent of pressure over this range. Since higher $[O_2]$ were employed in lower total pressure experiments, the k' from lower pressure experiments are larger than that of higher pressure experiments in Figure 4.

TABLE 1: Experimentally Determined Rate Coefficients at 289 K[a]

pressure (Torr)	rate constants: from k' vs $[O_2]$ data	from k' vs [NO] data	recommend value
	$CH_2ClO + O_2 \xrightarrow{k_5} HC(O)Cl + HO_2$[b]		
5	8.0×10^{-14}	8.09×10^{-14}	
10	8.0×10^{-14}	7.52×10^{-14}	
15	7.65×10^{-14}	8.09×10^{-14}	
20	8.29×10^{-14}	8.09×10^{-14}	
25	8.21×10^{-14}	8.09×10^{-14}	
30	7.23×10^{-14}	8.09×10^{-14}	
35	8.46×10^{-14}	7.42×10^{-14}	
average	$(8.0 \pm 0.8) \times 10^{-14}$		$(8.0 \pm 0.8) \times 10^{-14}$
	$CH_2ClO \xrightarrow{k_6} HCO + HCl$[c]		
5	230	257	244 ± 38
10	461	378	419 ± 117
15	691	608	650 ± 117
20	922	893	907 ± 41
25	1152	957	1055 ± 275
30	1381	1401	1392 ± 25
35	1613	1429	1521 ± 260
	$CH_2ClO + NO \xrightarrow{k_9} HC(O)Cl + HNO$[b]		
5	2.71×10^{-12}	2.67×10^{-12}	
10	2.71×10^{-12}	2.92×10^{-12}	
15	2.71×10^{-12}	2.86×10^{-12}	
20	2.71×10^{-12}	2.73×10^{-12}	
25	2.71×10^{-12}	2.57×10^{-12}	
30	2.71×10^{-12}	2.85×10^{-12}	
35	2.71×10^{-12}	2.42×10^{-12}	
average		$(2.7 \pm 0.4) \times 10^{-12}$	$(2.7 \pm 0.4) \times 10^{-12}$

[a] Uncertainties of k_5 and k_9 are 2σ standard deviations. Uncertainties of k_6 were determined by averaging the two values of k_6 at each total pressure. [b] Units of cm^3 $molecule^{-1}$ s^{-1}. [c] Units of s^{-1}.

TABLE 2: Experimentally Determine Rate Coefficients at 10 Torr and Different Temperatures

temp (K)	rate constants: from k' vs $[O_2]$ data	from k' vs [NO] data	recommend value
	$CH_2ClO + O_2 \xrightarrow{k_5} HC(O)Cl + HO_2$[a]		
265	6.11×10^{-14}	8.06×10^{-14}	$(6.1 \pm 2.0) \times 10^{-14}$
280	6.77×10^{-14}	7.34×10^{-14}	$(6.8 \pm 1.5) \times 10^{-14}$
289	$(8.0 \pm 0.8) \times 10^{-14}$	8.14×10^{-14}	$(8.0 \pm 0.8) \times 10^{-14}$
306	9.68×10^{-14}	8.71×10^{-14}	$(9.7 \pm 3.0) \times 10^{-14}$
	$k_5(T) = (2.0 \pm 0.7)\, e^{-(934 \pm 128)/T} \times 10^{-12}$ cm^3 $molecule^{-1}$ s^{-1}		
	$CH_2ClO \xrightarrow{k_6} HCO + HCl$[b]		
265	60	118	89 ± 40
280	371	381	376 ± 75
289	461	378	419 ± 117
306	1070	1139	1104 ± 97
	$k_{6,10\text{Torr}}(T) = (7.7 \pm 2.3)\, e^{-(4803 \pm 772)/T} \times 10^{9}$ s^{-1}		
	$CH_2ClO + NO \xrightarrow{k_9} HC(O)Cl + HNO$[a]		
265	2.9×10^{-12}	2.96×10^{-12}	2.96×10^{-12}
280	2.7×10^{-12}	2.63×10^{-12}	2.63×10^{-12}
289	2.7×10^{-12}	$(2.7 \pm 0.4) \times 10^{-12}$	$(2.7 \pm 0.4) \times 10^{-12}$
306	2.5×10^{-12}	2.41×10^{-12}	2.41×10^{-12}
average			$(2.7 \pm 0.6) \times 10^{-12}$

[a] Units of cm^3 $molecule^{-1}$ s^{-1}. [b] Units of s^{-1}.

The values of k_5 and k_9 obtained from the slopes of Figures 3 and 4 at different total pressures are listed in Table 1. Table 2 lists the 10 Torr values of k_5 and k_9 obtained from k' vs $[O_2]$ plots at 265 K, 280, 289, and 306 K. The reported uncertainties of k_5 and k_9 in Table 1 are 2σ standard deviations. An Arrhenius

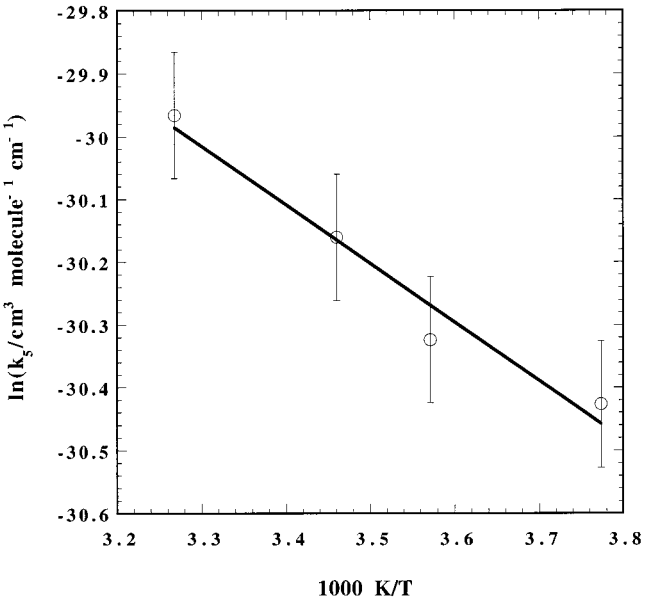

Figure 5. Arrhenius plot of experimentally determined k_5: ○, experimental data; —, linear fit. Data are taken from Table 2.

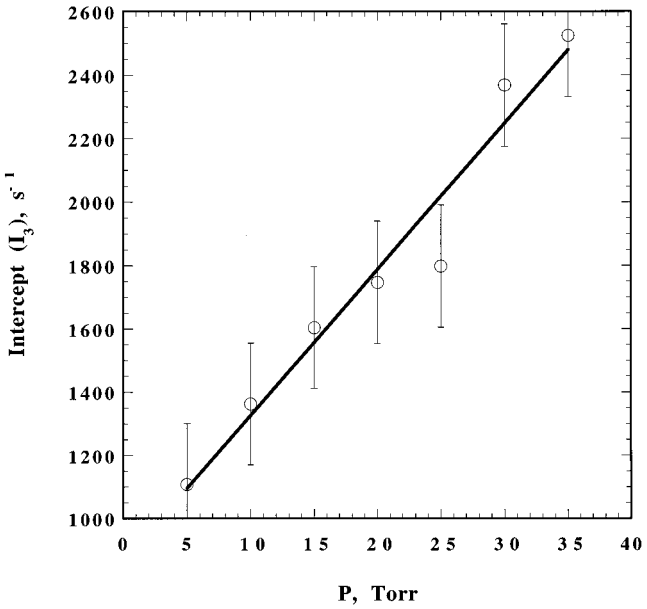

Figure 6. Intercept I_3 vs total pressure plot at 289 K. The intercepts are obtained from Figure 3; ○, experimentally determined data; —, linear fit.

plot of the values of k_5 obtained from k' vs $[O_2]$ plots is shown in Figure 5. The temperature dependence of k_5 is expressed in Arrhenius form by eq 18.

$$k_5(T) = (2.0 \pm 0.7) \times 10^{-12}\, e^{-(934\pm128)/T}\ cm^3\ molecule^{-1}\ s^{-1} \quad (18)$$

The values of k_9 listed in Table 2 show no discernible trend with temperature over the entire range. Any temperature dependence must be so weak that it is obscured by the experimental uncertainty. The average value of k_9, obtained by averaging all of the rate coefficients in Table 2., is given in eq 19.

$$k_9 = (2.7 \pm 0.6) \times 10^{-12}\ cm^3\ molecule^{-1}\ s^{-1} \quad (19)$$

Determination of k_6. The rate coefficient k_6 can be determined from the intercepts of Figures 3 and 4. The kinetic analysis predicts that the intercept of Figure 3, I_3, is

$$I_3 = k_6 + k_9\,[NO] \quad (20)$$

Since the NO partial pressure is kept constant in these experiments, k_9[NO] is a constant, since k_6 is a function of pressure. I_3 is also a function of pressure. Thus the intercept of a plot of I_3 vs P should give k_9[NO], and subtraction of this value of k_9[NO] from the value of I_3 at each pressure should give $k_6(P)$. Figure 6 shows the plot of I_3 vs P for the 289 K data of Figure 3. The intercept of this plot can be reliably determined, and after subtraction from I_3 gives the 289 K values of k_6 from 5 to 35 Torr. These values of k_6 are listed in Table 1. Ten Torr values of k_6 at 265, 280, 289, and 306 K, obtained in the same way, are in Table 2. An estimate of k_9 can be obtained from the intercepts of I_3 vs P plots and the measured [NO]. The values of k_9 determined in this way are listed in Table 1 for pressures from 5 to 35 Torr and 289 K, and in Table 2 for 10 Torr at each temperature. They are generally in excellent agreement with the values of k_9 obtained from the slopes of the k' vs [NO] plots, lending confidence to the kinetic analysis.

An alternative method for determination of k_6 is available from the k' vs [NO] data. The kinetic analysis predicts that the intercepts of the k' vs [NO] plots can be expressed as eq 21.

$$I_4 = k_6 + k_5[O_2] \quad (21)$$

Using the values of k_5 determined from k' vs $[O_2]$ plots, the known $[O_2]$ at the pressure of each series of experiments shown in Figure 4, and the intercepts from Figure 4, values of k_6 can be calculated from eq 21. The 289 K values of k_6 from 5 to 35 Torr are listed in Table 1, and the 10 Torr values at 265, 280, 289, and 306 K are listed in Table 2. They are in good agreement with the k_6 values determined from k' vs $[O_2]$ data.

Equation 21 can also be used to estimate k_5 if values of k_6 from k' vs $[O_2]$ data are used in conjunction with I_4. The values of k_5 so obtained are listed in Tables 1 and 2 under the heading "from k' vs [NO] data". They are in excellent agreement with values of k_5 from k' vs $[O_2]$ data and support the kinetic analysis. The final values of k_6 at 289 K are listed in Tables 3 and 1. Each entry is the average of two values, one obtained from the intercepts of Figure 3 (289 K) and the other from the intercepts of Figure 4 (289 K). The reported uncertainties of k_6 in Tables 1 and 2 were determined by averaging the two values of k_6 at each pressure and temperature, respectively. Note that the experimentally accessible pressure range for k_6 decreases with increasing temperature because of the time resolution limit of the apparatus for reliable determination of rate coefficients discussed above.

For experiments at other temperatures, k_5 and k_9 at 10 Torr were determined in the same manner as 289 K experiments. However, k_6 was obtained using intercepts (I_{10Torr},t) of k' vs $[O_2]$ plots at 10 Torr and different [NO]. The intercept of the I_{10Torr},t vs [NO] plot is equal to k_6 at 10 Torr and at that particular temperature. The values of the rate coefficients are listed in Tables 1 and 2.

Since 10 Torr is the only pressure for which a value of k_6 is available at each of the four temperatures, an Arrhenius plot of the 10 Torr data was prepared and is shown in Figure 7. A linear least-squares fit gives the 10 Torr Arrhenius expression of eq 22.

$$k_6(T)_{10Torr} = (7.7 \pm 2.3) \times 10^9\, e^{-(4803\pm722)/T}\ s^{-1} \quad (22)$$

TABLE 3: Experimentally Determined Rate Coefficients at 289 K (From k' vs [NO] Plot Data)

P (Torr)	I_4 (S^{-1})	$[O_2]^a$	$k_9{}^b$	$k_5{}^{c,d}$	$k_6{}^d$ (s^{-1})	$I_4 - k_6$ (s^{-1})	$k_5{}^c = (I_4 - k_6)/[O_2]$	$k_6 = I_4 - k_5[O_2]$
5	2537	2.85	2.67	8.0	230	2307	8.09	257
10	1762	1.73	2.92	8.0	461	1301	7.52	378
15	1752	1.43	2.86	7.65	691	1060	7.42	608
20	1797	1.13	2.73	8.29	922	875	7.75	893
25	1781	1.03	2.57	8.21	1152	629	6.11	957
30	2183	0.978	2.85	7.23	1383	801	8.19	1401
35	2446	1.20	2.42	8.46	1613	833	6.94	1429

[a] Units of 10^{16} molecule cm^{-3}. [b] Units of 10^{-12} cm^3 $molecule^{-1}$ s^{-1}. [c] Units of 10^{-14} cm^3 $molecule^{-1}$ s^{-1}. [d] From k' vs $[O_2]$ plot results.

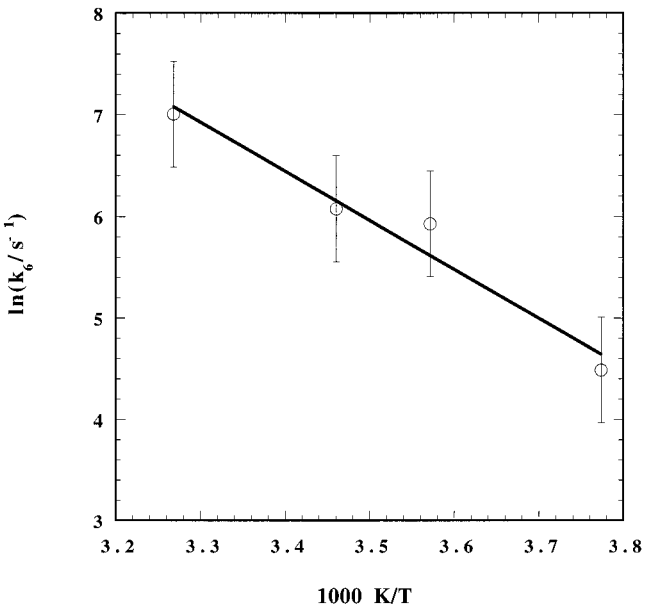

Figure 7. Arrhenius plot of experimentally determined k_6 at 10 Torr of total pressure: ○, experimentally determined data; — linear fit. Data are taken from Table 2.

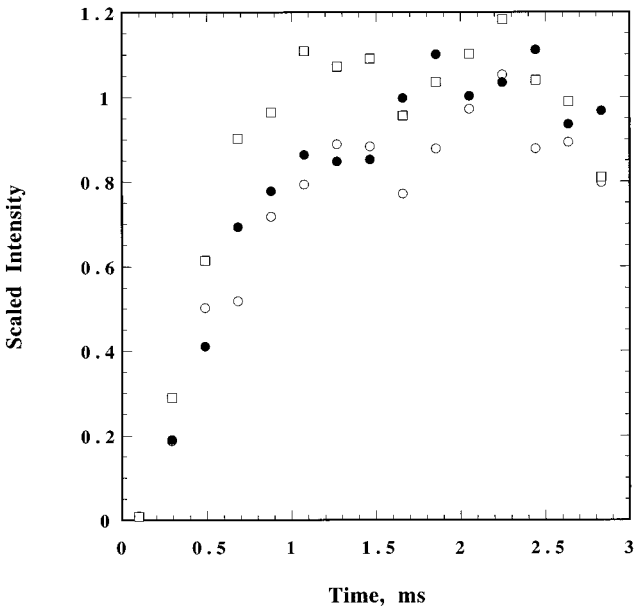

Figure 8. Experimentally detected kinetic signals of H_2O and NO_2 at 289 K and 20 Torr. Gas mixture, 25% CH_3Cl/3% O_2/NOCl/NO; ○, H_2O at $m/z = 18$; ●, NO_2 at $m/z = 46$.

The activation energy for this three-center elimination is seen to be quite small. The 10 Torr value, about 9.5 kcal/mol, is expected to be smaller than at the high-pressure limit, due to falloff effects. The very small value of the preexponential factor can also be accounted for by the falloff. The difference between $E_{a,6}$ reported here and the 700 Torr value of 8.6 ± 1.9 Kcal mol^{-1} given by Wallington et al.[8] is due to the approximate nature of their method of estimation.

Discussion

The HO_2 formed by reaction 5 can react with NO to form NO_2 and OH, which can further react with CH_3Cl to give the CH_2Cl radical.

$$HO_2 + NO \rightarrow NO_2 + OH \quad (23)$$

$$OH + CH_3Cl \rightarrow CH_2Cl + H_2O \quad (24)$$

Reactions 5, 23, 24, 3, and 8 comprise a chain reaction, with CH_2ClO as a chain carrier, in which reactions 6 and 9 are chain termination steps. In addition to reaction 2, a significant amount of CH_2Cl will be produced by reaction 24, if there are no other reactions which consume OH. In other words, formation of HCl and HC(O)Cl should continue for a long time if the chain reaction is not efficiently terminated. The experimentally measured growth curves of HCl and HC(O)Cl show that their formation is complete in about 2 ms, showing that a chain reaction is not important at reaction times longer than 2 ms.

Additional experimental work and a numerical study were done to gain more information about the possible influence of chain reactions. Formation signals of H_2O at $m/z = 18$ and NO_2 at $m/z = 46$ were recorded at 289 K and at 20 Torr total pressure (Figure 8). Although there is some scatter, the growth curves show that the formation of H_2O and NO_2 are completed in about the same time as that of formation of HCl and HC(O)Cl. There is no evidence that H_2O and NO_2 concentrations continue to increase, as would be expected if a chain reaction were important.

Parallel experiments were done using 25% CH_3Cl/2% O_2/N_2 and 25% CH_3Cl/2% O_2/10% CH_3CHO/N_2 gas mixtures, while the same concentration of NO/NOCl was introduced through the separate inlet. The CH_3CHO was added to scavenge OH, since the rate coefficient for reaction of OH with CH_3CHO is about 3 orders of magnitude larger than with CH_3Cl. More than 99% of the OH formed by reaction 23 will be consumed by reaction 25 instead of reaction 24.

$$OH + CH_3CHO \rightarrow CH_3CO + H_2O \quad (25)$$

The growth curves of HCl and HC(O)Cl from these parallel experiments should be significantly different if OH plays an important role in their rate of formation. The experimental results in Figure 9 show that the growth curves of HCl and HC(O)Cl were indistinguishable. The lack of any dependence of the growth curves on added CH_3CHO argues against the importance of the chain reaction during this stage of the reaction.

A 36-step reaction model was used to predict profiles of HCl, HC(O)Cl, H_2O, NO_2, OH, and HO_2. The reaction mechanism and rate coefficients are listed in Table 4. The rate coefficients for the numerical simulations were taken from the literature,

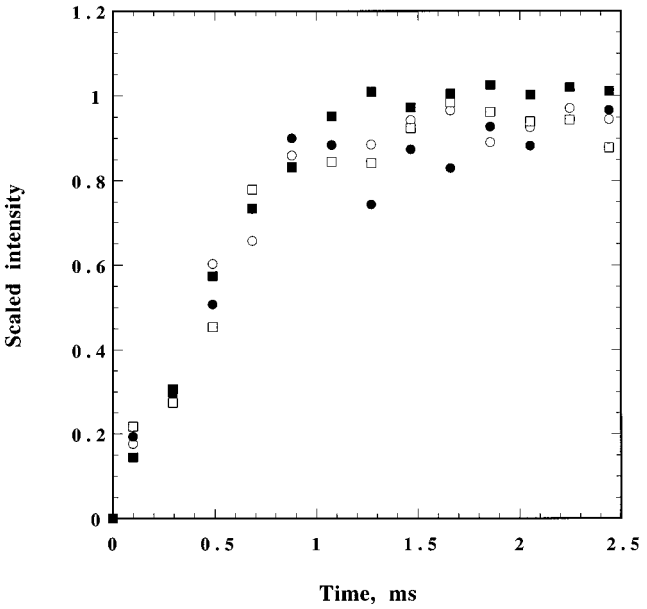

Figure 9. Experimentally detected kinetic signals of HC(O)Cl and HCl for different gas mixture systems and at 20 Torr and 289 K. 25% CH_3Cl/3% O_2/NOCl/NO: ○, $m/z = 64$; □, $m/z = 36$. 25% CH_3Cl/3% O_2/10% CH_3CHO/NOCl/NO: ●, $m/z = 64$; ■, $m/z = 36$.

except k_5, k_6, and k_9, which were the experimentally determined values from this work. The calculated profiles of HCl, HC(O)Cl, H_2O, and NO_2 (Figure 10.1) have about the same shape and rise time as the experimental growth curves. Also, the calculated results show there is no significant amount of OH and HO_2 (Figure 10.2) present after 2 ms. Calculated concentration time curves of HC(O)Cl and HCl were used to make $\ln(1 - [HC(O)Cl]/[HC(O)Cl])_\infty$ vs time plots and $\ln(1 - [HCl]/[HCl])_\infty$ vs time plots. The plots were linear, showing that the mechanism predicts pseudo-first-order decay of CH_2ClO, in support of the kinetic analysis. A chain reaction would regenerate CH_2ClO and give noticeable nonlinearity to the calculated semilog plots. Furthermore, the semilog plots for HC(O)Cl and HCl yielded almost overlapping straight lines, as predicted by the kinetic analysis.

The above experiments and numerical simulations show that a chain reaction involving OH does not have a significant influence on the rate of formation of HCl and HC(O)Cl. This is most likely due to the removal of CH_2ClO radicals by reactions 6 and 9 and to the removal of OH by other reactions which compete with CH_3Cl.

The slope of the calculated semilog plots is equal to the pseudo-first-order rate coefficient, k'_{calc}. This may be compared with the experimentally determined pseudo-first-order rate coefficient, k'_{exp}. The difference between k'_{cal} and k'_{exp} was used to calculate the relative deviation, $\sigma = 100 \times (k'_{exp} - k'_{cal})/k'_{exp}$, which is a measure of the goodness of the mechanism. At 289 K the mechanism does a very good job since σ was calculated to be 3.1% at 5 Torr and 2.8% at 20 Torr. At 306 K the values of σ were somewhat larger, 19.8% (5 Torr) and 17.5% (10 Torr), but still commensurate with the statistical uncertainties in the experimental data. However, at 265 K, $\sigma = 43\%$ (5 Torr) and 68% (20 Torr) and the mechanism does not do quite as

TABLE 4: Reaction Mechanism for Numerical Simulation (289 K, 20 Torr)[a]

entry	reaction	k (cm^3 $molecule^{-1}$ s^{-1})	ref
2	$Cl + CH_3Cl \rightarrow CH_2Cl + HCl$	4.37×10^{-13}	26
3	$CH_2Cl + O_2 + M \rightarrow CH_2ClO_2 + M$	6.13×10^{-13}	36
4	$2CH_2ClO_2 \rightarrow 2\ CH_2ClO + O_2$	3.72×10^{-12}	37
5	$O_2 + CH_2ClO \rightarrow HC(O)Cl + HO_2$	8.0×10^{-14}	this work
6	$CH_2ClO + M \rightarrow HCl + CHO + M$	$907\ s^{-1}$	this work
8	$CH_2ClO_2 + NO \rightarrow CH_2ClO + NO_2$	1.99×10^{-11}	26
9	$CH_2ClO + NO \rightarrow HNO + HC(O)Cl$	2.7×10^{-12}	this work
23	$HO_2 + NO \rightarrow OH + NO_2$	8.79×10^{-12}	26
24	$CH_3Cl + OH \rightarrow CH_2Cl + H_2O$	3.15×10^{-14}	26
27	$CH_2ClO_2 + HO_2 \rightarrow O_2 + HC(O)Cl + H_2O$	1.52×10^{-11}	38
28	$CH_2ClO_2 + HO_2 \rightarrow O_2 + CH_2ClOOH$	5.63×10^{-12}	26
29	$2HO_2 \rightarrow O_2 + H_2O_2$	1.83×10^{-12}	26
30	$O_2 + HCO \rightarrow HO_2 + CO$	5.68×10^{-12}	26
31	$Cl + CH_2ClO_2 \rightarrow CH_2ClO + ClO$	7.7×10^{-11}	26
32	$Cl + CH_2ClO_2 \rightarrow HCl + CHClO_2$	7.4×10^{-11}	26
33	$CH_2ClO_2 + ClO \rightarrow CH_2ClO + ClOO$	1.73×10^{-12}	26
34	$Cl + HO_2 \rightarrow HCl + O_2$	3.24×10^{-11}	26
35	$OH + Cl_2 \rightarrow Cl + HOCl$	6.22×10^{-14}	26
36	$CH_2Cl + Cl_2 \rightarrow CH_2Cl_2 + Cl$	2.73×10^{-13}	39
37	$HCO + Cl_2 \rightarrow H\ C(O)Cl + Cl$	5.57×10^{-12}	40
38	$Cl + NOCl \rightarrow Cl_2 + NO$	8.2×10^{-11}	26
39	$OH + HO_2 \rightarrow H_2O + O_2$	1.14×10^{-10}	26
40	$OH + OH \rightarrow H_2O + O$	1.83×10^{-11}	26
41	$OH + ClO \rightarrow pr\ oduct$	1.67×10^{-11}	26
42	$OH + NO + M \rightarrow HONO + M$	4.24×10^{-13}	26
43	$HO_2 + NO_2 + M \rightarrow HO_2NO_2 + M$	1.14×10^{-13}	26
44	$OH + NO_2 + M \rightarrow HNO_3 + M$	1.45×10^{-12}	26
45	$OH + HCl \rightarrow H_2O + Cl$	7.75×10^{-13}	26
46	$OH + HONO \rightarrow H_2O + NO_2$	4.67×10^{-12}	26
47	$OH + NOCl \rightarrow NO + HOCl$	1.8×10^{-13}	41
48	$OH + NOCl \rightarrow Cl + HNO_2$	3.07×10^{-13}	41
49	$OH + HOCl \rightarrow H_2O + ClO$	5.32×10^{-13}	26
50	$OH + H_2O_2 \rightarrow H_2O + HO_2$	1.67×10^{-12}	26
51	$HO_2 + Cl \rightarrow OH + ClO$	8.64×10^{-12}	26
52	$HO_2 + ClO \rightarrow HOCl + O_2$	5.41×10^{-12}	26
53	$NO + ClO \rightarrow NO_2 + Cl$	1.75×10^{-11}	26

[a] Initial concentrations (molecule cm^{-3}): CH_3Cl, 1.67×10^{17}; O_2, 1.13×10^{16}; Cl, 6.69×10^{14}; NOCl, 3.34×10^{16}; NO, 3.34×10^{14}.

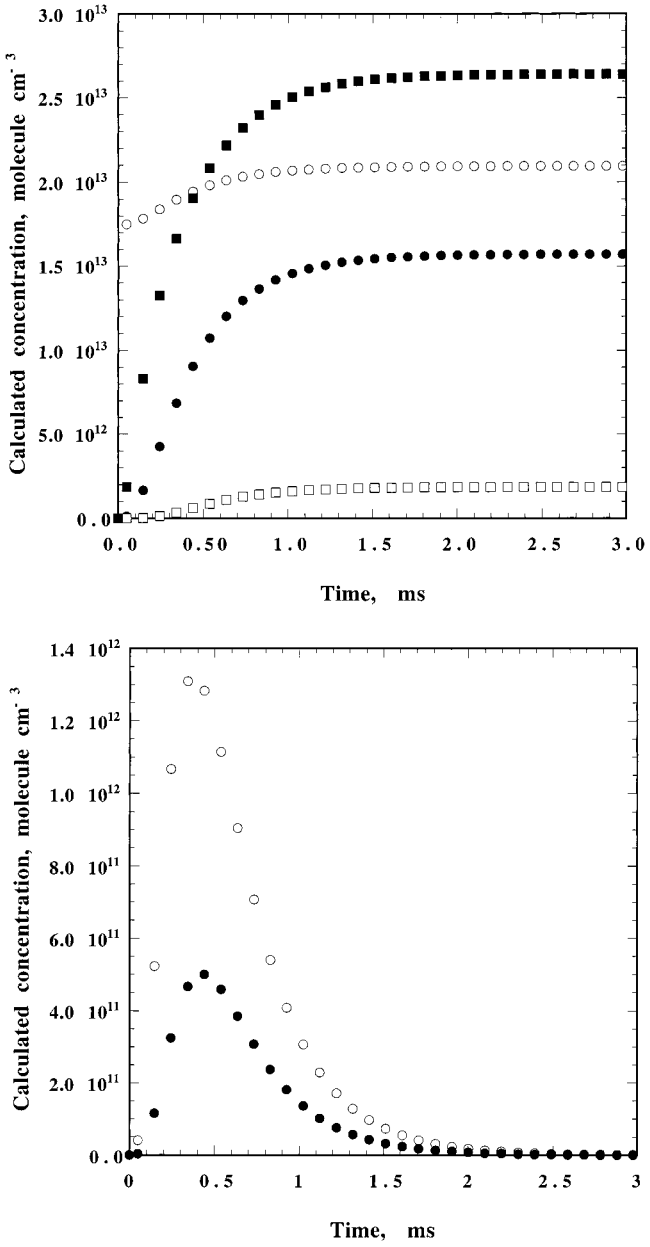

Figure 10. Calculated profiles of various species at 289 K and 20 Torr. Reaction mechanism and concentrations are listed in Table 4. (10.1) ○, HCl; ●, HC(O)Cl; □, H_2O; ■, NO_2. (10.2) ○, HO_2; ●, OH.

well here. The reason for the divergence at low temperature is not apparent, although it should be noted that the literature values of the rate coefficients are generally not as well established at lower temperatures as they are near room temperature.

Bilde et al.[16] have recently reported evidence that the a portion of the CH_2ClO radicals formed in reaction 8 are chemically activated and that they are sufficiently energetic to eliminate HCl.

$$CH_2ClO_2 + NO \rightarrow CH_2ClO^* + NO_2 \qquad (8a)$$

The asterisk denotes the chemically activated radical. This is in contrast with CH_2ClO formed by the CH_2ClO_2 self-reaction, which is less exothermic and probably does not produce a chemically activated product. Any CH_2ClO^* formed in our experiments will not affect the observed kinetics, since it will not be present at our millisecond reaction times. Reaction 8a would generate CH_2ClO^* on a submillisecond time scale, and energy states above the HCl elimination threshold energy would have to have lifetimes that are orders of magnitude shorter than milliseconds if they are able to compete with collisional deactivation at the pressures of our experiments. Any HCl coming from this source would appear with prompt HCl from reaction 2 in the first channel of the multichannel analyzer. The quantitation of prompt HCl, which might be able to distinguish whether any HCl in excess of that from reaction 2 is present, was not attempted in these experiments. Additional work to address this point is planned for the near future.

Any chemically activated CH_2ClO formed by reaction 8 will not survive to influence events occurring after 1 ms. At the pressures of these experiments, CH_2ClO^* would become thermalized by the more than 10^4 collisions that it would suffer in a millisecond. Thus, all rate coefficients determined here are for thermalized species. Table 2 and Figure 5 show that the values of k_5 determined from the slope of k' vs $[O_2]$ plots and from the intercept of k' vs [NO] plots are in good agreement. Table 2 also shows that the values of k_9 by the two different methods are in good agreement at every temperature. The values of k_5 and k_9 from the slopes of the k' vs $[O_2]$ and k' vs [NO] plots, respectively, are considered to be more reliable than values taken from the intercept, since each intercept is only a single data point, whereas several experiments are involved in each slope. Furthermore, the least-squares analysis of the slopes affords determination of statistical uncertainties. Thus, we recommend the rate coefficients derived from the slopes as the best values of k_5 and k_9, with the values from the intercepts corroborating the kinetic analysis.

The values of k_6 are in good agreement with the results from our previous study at 306 K.[10] In that work, Cl_2 was the source of Cl, CH_2ClO was generated by self-reaction of CH_2ClO_2 radicals, and the rate coefficients were determined by nonlinear regression of the 18-step reaction mechanism on HCl growth data. The two previously reported values of k_6 in Table 2 of ref 10 are 920 and 995 s^{-1} at 10 Torr, in good agreement (within statistical uncertainty) with $k_6(306\ K) = (1104 \pm 97)\ s^{-1}$ reported here. Comparison of $k_5(306\ K) = (2.8 \pm 1.2) \times 10^{-13}$ cm^3 $molecule^{-1}$ s^{-1} from that work with the mean value calculated from eq 18, $k_5(306\ K) = (9.7 \pm 3.0) \times 10^{-14}$ cm^3 $molecule^{-1}$ s^{-1}, shows that the agreement is less good, although it is close to being within the statistical uncertainties. There are no literature values of k_9 with which to compare these results. Since the method of initiating the reaction and generating CH_2ClO_2 and the method of the kinetic analysis are both different, the closeness of the values of k_5 and k_6 from our previous study[10] with the values reported here is satisfying. Since the present kinetic analysis depends on the observed pseudo-first-order growths, whereas the analysis in ref 10 depends on regression of the data on a mechanism, the rate coefficients reported here are to be preferred.

Reaction 6 is very close to the low-pressure limit. This is first of all suggested by the apparent linearity of the data plotted in Figure 11, which shows the pressure dependence of k_6 at 289 K. Further evidence is obtained by empirical fitting. The solid line in Figure 11 is a nonlinear Troe curve fit.[17] The near linearity of the fit is also indicative that reaction 6 is very close to the low-pressure limit at the pressures of this investigation. The value of $k_{6,0}$, one of the parameters of the fit, is given by eq 26.

$$k_{6,0}(289\ K) = (1.4 \pm 0.4) \times 10^{-15}\ cm^3\ molecule^{-1}\ s^{-1} \qquad (26)$$

If this is multiplied by the 289 K total molecular concentration at a particular pressure, the experimentally measured values of k_6 are recovered. For example, at 10 Torr, $k_{6,0}[M] = 465\ s^{-1}$,

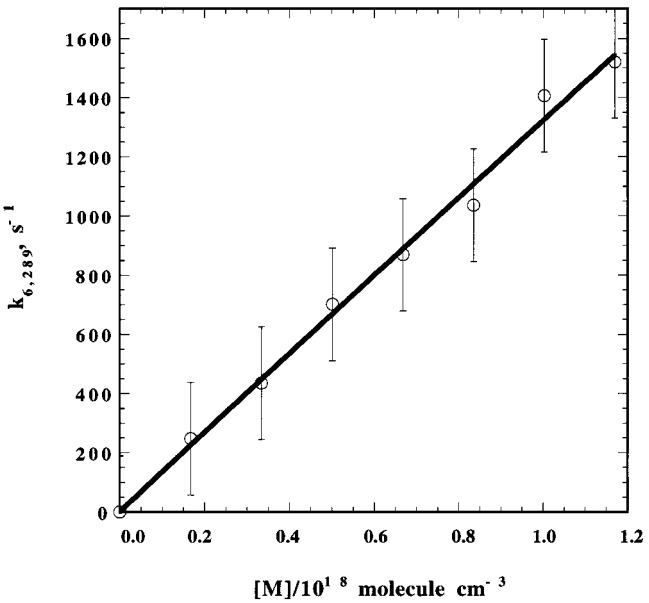

Figure 11. Pressure dependence of k_6 at 289 K: ○, experimentally determined data; —, linear fit. Data are taken from Table 1.

compared with the experimental value, 419 s^{-1}. The value of $k_{6,\infty}$(289 K) from the Troe fit is not reported here, because the long extrapolation makes it unreliable. More extensive use was not made of Troe fits since an RRKM analysis has been done and is being prepared for publication.[18]

The activation energy of reaction 5, 1.86 kcal/mol, is small and not dissimilar from the activation energies reported for direct kinetics studies of other oxy radical reactions with O_2 at temperatures below 500 K. For the $CH_3O + O_2$ reaction, activation energies of 2.6[19] and 2 kcal/mol[20] have been reported. For $C_2H_5O + O_2$,[21] $E_a = 1.1$ kcal/mol; for iso-$C_3H_7O + O_2$,[22] $E_a = 0.4$ kcal/mol; and for $CFCl_2CH_2O$,[23] $E_a = 1.8$ kcal/mol. Wantuck et al.[24] found curvature of the Arrhenius plot for CH_3O+O_2 over the temperature range 298−973 K, indicative of higher energy channels becoming important at higher temperatures. The preexponential factors for the alkoxy radicals are in the 10^{-14} cm^3 $molecule^{-1}$ s^{-1} range, and for $CFCl_2CH_2O$, $A = 2.4 \times 10^{-15}$ cm^3 $molecule^{-1}$ s^{-1}. These *A*-factors are too small to be consistent with direct H-atom transfer to O_2. They have given rise to discussion of mechanism, particularly the nature of the transition state, which is required to be somewhat less entropic than the typical H-atom metathesis transition state.[25] Since $A_5 = 2 \times 10^{-12}$ cm^3 $molecule^{-1}$ s^{-1}, reaction 5 is different than these $RO+O_2$ reactions. While preexponential factors for H-atom metathesis can be smaller than the *A*-factor of reaction 5, there are good examples of metathesis reactions with similar preexponentials. For example, H-atom transfer from small molecules to OH commonly have Arrhenius preexponential factors in the 10^{-12} cm^3 $molecule^{-1}$ s^{-1} range,[26] and these reactions are usually considered to occur directly through linear transition states. Thus there is no compelling need to rationalize reaction 5 as occurring through a tighter and therefore less entropic transition state. Jungkamp and Seinfeld[27] have carried out ab initio and density functional calculations of the $CH_3O + O_2$ reaction, finding that the barrier for trioxy formation is lower than the barrier for direct H-atom transfer and that unimolecular decomposition of CH_3OOO via a cyclic transition state is the dominant path for formation of HO_2 and CH_2O. Substitution of Cl for H in CH_3O is expected to decrease the energy of the remaining two C−H bonds. If this lowers the barrier for direct transfer sufficiently, it is possible that direct transfer would become the dominant reaction path for reaction of O_2 with CH_2ClO and that the mechanism would not involve formation and rearrangement of an intermediate complex. This might explain the larger preexponential factor (compared with $CH_3O + O_2$). An ab initio study would be expected reveal whether this is the case.

The following four channels for the reaction of CH_2ClO with NO are considered here:

$$CH_2ClO + NO \rightarrow CH_2ClONO \quad (9a)$$

$$CH_2ClO + NO \rightarrow HC(O)Cl + HNO \quad (9b)$$

$$CH_2ClO + NO \rightarrow CH_2ClNO_2 \quad (9c)$$

$$CH_2ClO + NO \rightarrow CH_2Cl + NO_2 \quad (9d)$$

Of these, reaction 9d is too endothermic to be important at the temperatures employed in this work. The observation of HC(O)Cl confirms the occurrence of disproportionation (reaction 9b), and although CH_2ClONO was not detected, in view of the importance of methyl nitrite formation in the $CH_3O + NO$ reaction, it seems highly likely that the combination channel, reaction 9a, is also open. While reaction 9c cannot be ruled out, it probably requires a three-center transition state, and if so, it would have a smaller *A*-factor than simple combination. Regardless of the operative reaction channels, eqs 16 and 17 show that the kinetic analysis gives the overall rate coefficient, k_9, and not k_{9b}, the rate coefficient for the observed channel.

To our knowledge, there are no literature values of k_9 with which to compare our results. Table 2 shows that k_9 is remarkably insensitive to variations of temperature and pressure. The temperature insensitivity is similar to the $CH_3O + NO$ reaction. From a study of the pyrolysis of CH_3ONO, He et al.[28] found that the reaction of CH_3O with NO had an activation energy of 0 ± 200 cal/mol. At somewhat lower temperatures, McCaulley et al.[29] and Frost and Smith[30] report small negative temperature coefficients. Their work was done over wider temperature ranges, 220−473 and 296−573 K, respectively, than the 265−306 K range of this work. However, the absence of any pressure dependence of k_9 is in contrast with $CH_3O + NO$, which is known to increase in rate with increasing pressure.[31−33] Direct experiments have shown that the rate coefficient increases as pressure increases from a few Torr to the vicinity of 100 Torr.[29,30,34,35] The pressure dependence must be attributed to formation of a chemically activated methyl nitrite intermediate, but the literature differs on whether the reaction all goes through the intermediate, as in the scheme below,[30] or whether there is an accompanying pressure-independent path.[29] Dóbé et al. have claimed that it is not possible to distinguish alternate pathways from the pressure dependence of the rate coefficient alone.[35]

$$CH_3O + NO \leftrightarrow CH_3ONO^* \rightarrow CH_2O + HNO$$
$$\downarrow +M$$
$$CH_3ONO$$

If $CH_2ClO + NO$ were to occur through CH_2ClONO^*, the failure to observe any pressure dependence of k_9 would have to be explained by the association being very close to the high-pressure limit at the pressures of our experiments. Reaction 9 is expected to be closer to the high-pressure limit than $CH_3O + NO$ due to the larger vibrational state density of CH_2ClONO^* (compared with CH_3ONO^*), but near the high-pressure limit, the yield of HC(O)Cl would be very small if the above scheme holds. The pressure independence of k_9 could also be explained if the mechanism is direct transfer of an H-atom from CH_2ClO

to NO. Since $E_9 \approx 0$, k_9 could then be associated with $A_9 = 3.1 \times 10^{-12}$ cm^3 molecule^{-1} s^{-1}, which is in the normal range for H-atom metathesis between polyatomic and diatomic reactants.[25] Further work will be needed to clarify the mechanism of reaction 9.

Kaiser and Wallington[7] have shown that the reaction of CH_2ClO with O_2 is the dominant path for its removal from the atmosphere. The results of this study confirm that conclusion. At ground level, where temperature and pressure are taken to be 300 K and 1 atm, respectively, the relative rate of reactions 6 and 5 is given by $r_6/r_5 = k_6/k_5[O_2]$. Calculating k_5 from eq 18 and extrapolating k_6 linearly from the 10 Torr and 306 K value in Table 2 to 760 Torr gives $r_6/r_5 = 0.14$. At the tropopause, where conditions are approximately 200 K and 100 Torr, the ratio $r_6/r_5 = 1.7 \times 10^{-4}$ was calculated. Linear extrapolation of k_6 leads to an overestimate at higher pressures because the slope of k_6 vs P decreases with increasing pressure in the falloff. The actual values of r_6/r_5 at the surface and at the tropopause will be somewhat smaller than the calculated ratios. Since k_9 is approximately a factor of 30 larger than k_5, reaction 9 cannot be important, even in highly polluted areas, since NO_x concentrations are orders of magnitude smaller than O_2 concentrations.

Acknowledgment. This research was supported by NASA Upper Atmosphere Research Program under the grant NASA/NAG5-3980.

References and Notes

(1) Senkan, S. M. U. S. Patent 07/040853, 1987.
(2) Granada, A.; Karra, S. B.; Senkan, S. M. *Ind. Eng. Chem. Res.* **1987**, *26*, 1901.
(3) Wayne, R. P. *Chemistry of Atmospheres*, 2nd ed.; Oxford University Press: Oxford, 1991; p 135.
(4) *Atmospheric Ozone*, WMO Report No. 16, 1985, p 642.
(5) Sanhueza, H.; Heicklen, J. *J. Phys. Chem*. **1975**, *79*, 7.
(6) Niki, H.; Maker, P. D.; Savage, C. M.; Breitenbach, L. P. *I. J. Chem. Kinet*. **1980**, *12*, 1001.
(7) Kaiser, E. W.; Wallington, T. J. *J. Phys. Chem*. **1994**, *98*, 5679.
(8) Wallington, T. J.; Orlando, J. J.; Tyndall, G. S. *J. Phys. Chem*. **1995**, *99*, 9437.
(9) Catoire, V. A.; Lesclaux, R.; Lightfoot, P. D.; Rayez, M. T. *J. Phys. Chem*. **1994**, *98*, 2889.
(10) Wu, F.; Carr, R. W. *Chem. Phys. Lett.* **1999**, *305*, 44.
(11) Moore, S. B.; Carr, R. W. *J. Phys. Chem.* **1990**, *94*, 1393.
(12) Wu, F.; Carr, R. W. *Int. J. Chem. Kinet*. **1991**, *23*, 701.
(13) Moore, S. B.; Carr, R. W. *Int. J. Mass Spectrosc. Ion Phys.* **1977**, *24*, 161.
(14) Hutton, E.; Wright, M. *J. Chem. Soc., Faraday Trans.* **1965**, *61*, 78.
(15) Wu, F.; Carr, R. W. *J. Phys. Chem*. **1995**, *99*, 3128.
(16) Bilde, M.; Orlando, J. J.; Tyndall, G. S.; Wallington, T. J.; Hurley, M. D.; Kaiser, E. W. *J. Phys. Chem.* **1999**, *103*, 3963.
(17) Troe, J. *Phys. Chem*. **1979**, *83*, 114.
(18) Wu, F.; Carr, R. W. To be published.
(19) Gutman, D.; Sanders, N.; Butler, J. E. *J. Phys. Chem.* **1982**, *86*, 66.
(20) Lorenz, K.; Rhäsa, D.; Zellner, R. *Ber. Bunsen-Ges. Phys. Chem.* **1985**, *89*, 341.
(21) Hartmann, D.; Karthäuser, J.; Sawerysyn, J. P.; Zellner, R. *Ber Bunsen-Ges. Phys. Chem.* **1990**, *94*, 639.
(22) Balla, R. J.; Nelson, H. H.; McDonald, J. R. *Chem. Phys.* **1985**, *99*, 323.
(23) Wu, F.; Carr, R. W. *J. Phys. Chem.* **1996**, *100*, 9352.
(24) Wantuck, P. J.; Oldenborg, R. C.; Baughcum, S. L.; Winn, K. R. *J. Phys. Chem.* **1987**, *91*, 4653.
(25) Benson, S. W. *Thermochemical Kinetics*, 2nd ed.; Wiley-Interscience: New York, 1976, p 156−160.
(26) DeMore, W. B.; Sander, S. P.; Golden, D. M.; Hampson, R. F.; Kurylo, M. J.; Howard, C. J.; Ravishankara, A. R.; Kolb, C. E.; Molina, M. J. *Chemical Kinetics and Photochemical Data for Use in Stratospheric Modeling*, JPL Publication 1997, pp 97−94.
(27) Jungkamp, T. P. W.; Seinfeld, J. H. *Chem. Phys Lett.* **1996**, *263*, 371.
(28) He, Y.; Sanders, W. A.; Lin, M. C. *J. Phys. Chem.* **1988**, *92*, 5474.
(29) McCaulley, J. A.; Moyle, A. M.; Golde, M. F.; Anderson, S. M.; Kaufman, F. J. *J. Chem. Soc., Faraday Trans*. **1990**, *86*, 4001.
(30) Frost, M. J.; Smith, I. W. M. *J. Chem. Soc., Faraday Trans*. **1990**, *86*, 1757.
(31) Steacie, E. W. R.; Calder, D. S. *J. Chem. Phys.* **1936**, *4*, 96.
(32) Batt, L.; Milne, R. T.; McCulloch, R. D. *Int. J. Chem. Kinet.* **1977**, *9*, 567.
(33) Batt, L.; Rattray, G. N. *Int. J. Chem. Kinet.* **1979**, *11*, 1183.
(34) Zellner, R. *J. Chim. Phys.* **1987**, *84*, 403.
(35) Dóbé, S.; Lendvay, G.; Szilagyi, I.; Berces, T. *Int. J. Chem. Kinet*. **1996**, *26*, 887.
(36) Maricq, M. M.; Szente, J. J.; Kaiser, E. W.; Shi, J. *J. Phys. Chem.* **1994**, *98*, 2083.
(37) Catoire, V. A.; Lesclaux, R.; Lightfoot, P. D.; Rayez, M. T. *J. Phys. Chem.* **1994**, *98*, 2889.
(38) Wallington, T. J.; Hurley, M. D.; Schneider, W. F. *Chem. Phys. Lett.* **1996**, *251*, 164.
(39) Seetula, J. A.; Gutman, D.; Lightfoot, P. D.; Rayes, M. T.; Seakau, S. M. *J. Phys. Chem*. **1991**, *95*, 1068.
(40) Timonen, R. S.; Ratajczak, E.; Gutman, D. *J. Phys. Chem*. **1988**, *92*, 651.
(41) Abbatt, J. P. D.; Toohey, D. W.; Fenter, F. F.; Stevens, P. S.; Brune, W. H.; Anderson, J. G. *J. Phys. Chem*. **1989**, *93*, 1022.